Towards an Understanding of the Interactions Between Migrating Neural Crest Cells and Substrate Bound Guidance Molecules

Neural crest cell migration serves as a model system to study how the interactions of individual cells with their neighbors and their environment contributes to the guidance of migrating cell populations in the vertebrate embryo. In order to study how cells respond to cues from their environment, we cultured neural crest cells on patterned *in vitro* substrates to present the cells with a choice between migration on two different substrates, while simultaneously imaging the cell behavioral responses to these substrates.

In the course of developing this assay system, we developed improved methods for long-term imaging of fluorescent proteins with a confocal laser scanning microscope. We also tested a range of culture chambers for keeping neural crest cells healthy and developing normally on a microscope stage, and simplified the neural tube explant culture protocols.

To test the interactions of migrating neural crest cells with ephrin-B ligands, we generated patterns of ephrin-B protein on substrates coated in fibronectin and imaged the resulting cellular response to these patterns. We developed a novel photolithographic patterning method for building patterns of proteins on glass, and compared that to more established adsorption based methods. We found that our patterns were sharper and more robust, and that neural crest cells are generally repelled by ephrin-B ligands, in accordance with previous studies [1, 2]. However, the variation between individual neural crest cells and between cultures was too great to permit strong conclusions to be drawn. Since we greatly increased reduced the variation in implementation of the migration assay, but the variability in the cell behavior persisted, we conclude based on these experiments that the variability in the cellular response is due to differences inherent in the neural crest cells themselves and how different neural crest cells interpret the same guidance cue. We finish by discussing the basis for this variability and by discussing possible future directions for this type of experimental paradigm.

Andrew J. Ewald and Scott E. Fraser

Biological Imaging Center

California Institute of Technology

Background and Significance

The neural crest is a transitory, embryonic population of cells that emerges from the dorsal neural tube of vertebrate embryos in an anterior to posterior wave of migration that gives rise to a diverse range of derivatives, including neurons, glia, bone, cartilage, smooth muscle cells, melanocytes, among others [3-7]. Neural crest cells migrate over hundreds of microns in stereotypic patterns according to their level of origin in the anterior-posterior (A-P) axis, and each A-P level has a different mix of characteristic derivatives. As they migrate, at least some neural crest cells are individually multipotent, capable of giving rise to descendants in multiple locations and of multiple cell types, including both neurons and glia [8, 9]. It is a matter of controversy within the field whether a subpopulation of neural crest cells are more restricted in their developmental potential. Excellent reviews cover both sides of this discussion [4, 5].

We are interested in determining the factors that guide crest cells to their eventual destinations. Classical studies have shown that neural crest cells follow stereotyped migration patterns based on the location of origin of the crest within the neural tube, reviewed in [7]. An interesting example of these patterns occurs in the trunk of the developing avian spinal cord. Crest cells in this region migrate in a segmental fashion, always migrating through the anterior and not the posterior half of the adjacent somite pairs. This segmental pattern is conferred by the mesodermal tissue through which the cell migrates, not by the location of origin of the crest cells themselves, as surgical rotation of the mesoderm results

in a corresponding rotation in the segmental pattern [10]. We wanted to connect this observed migration pattern with the molecular factors and cellular rules which generate it.

Many candidate mechanisms have been proposed to guide neural crest cells. Cells could be following guidance cues that are diffusible, in the extracellular matrix, or bound to the plasma membranes of other cells. Crest cell migration might be driven by population pressure inside the neural tube, or cells may be actively following a gradient of chemoattractant originating outside of the neural tube. It is comparatively easy to propose a possible mechanism for crest cell guidance; the difficulty lies in developing an experimental approach that will distinguish between different candidate mechanisms within the full complexity of the developing embryo. Rather than try to solve the whole problem at once, several groups have attempted to develop *in vitro* migration assay systems to allow candidate molecules and tissues to be individually evaluated for their effects on crest cell migration.

Intense research has focused on the molecular or physical origin of the segmental migration of trunk neural crest cells. Work prior to 1997 chiefly focused on the role of extracellular matrix differences in guiding the neural crest, reviewed in [11, 12]. Many molecular differences were discovered between the rostral and caudal half somite. Molecules that have been observed in the correct time and place to be involved in trunk neural crest guidance include chondroitin

sulfate proteoglycans such as versican [13], N-Cadherin, Cad7, Cad6b [14], RhoB [15], F-spondin [16], Collapsin-1 (a semaphorin) [17], MMP2 [18], and peanut agglutinin binding molecules [19]. Following the report of the repulsive effect of Eph/ephrin signaling on migrating trunk neural crest cells [1, 2], much of the attention of the field turned in this direction.

It has been shown that neural crest cells avoid regions of a culture dish which contain ephrin-B1, and that disruption of ephrin-B1 signaling results in crest cells migrating through the posterior half of the somite [1,2]. It has also been shown that neural crest cells migrate through regions that are low in F-Spondin expression and avoid areas that highly express F-Spondin [16]. Furthermore, disruption of F-Spondin function with neutralizing antibodies is sufficient to allow neural crest cells to migrate into regions they would normally avoid [16]. It is not easy to reconcile these results. They appear to show that two unrelated molecules are each independently sufficient to establish permissive and repulsive neural crest migration zones within the embryo, while at the same time implying that disruption of either one will convert the repulsive zones into permissive zones.

It is difficult to reconcile these experiments because the assays used were designed to classify molecules as either repressive or permissive. It is clear from these papers alone that neural crest cell migration is influenced by many, different factors. If we want to understand migration guidance, we need to move

beyond a binary classification of molecules as permissive or inhibitory and instead try to compare the ways in which different signals affect neural crest cells, alone and in combination, in the hope that we will then be better able to understand how these signals will interact *in vivo*. I sought to build *in vitro* assays general enough to be capable of eventually distinguishing between the influences of each of these molecules, but focused experimentally on the effects of Eph/ephrin signaling on the neural crest. Once we characterized the response of neural crest cells to ephrin ligands, we planned a quantitative, combinatorial evaluation of the effects of other guidance molecules, both alone and in combinations.

Eph/ephrin Background

The Eph proteins are a family of receptor tyrosine kinases, with a cognate family of ligands, whose actions are implicated in the control of a variety of embryonic processes [20-23]. One of the first *in vivo* roles discovered for the Eph/ephrin family was in the topographic projection of retinal axons to the tectum [24]. This role was first identified through a series of choice assays developed by Friedrich Bonhoeffer and colleagues, which involved allowing axons from different regions of the retina to choice between crude membrane fragments [25]. They then modified the assay to present axons with a choice between ever purer membrane fractions until they were able to demonstrate that the repulsive activity was replicated purified ephrin proteins [24]. Similar assays were used to demonstrate a role for Eph/ephrin signaling in mouse [1] and chick [1, 2, 26]

neural crest cell migration. Different assays established the role of Eph/ephrin signaling in frog neural crest cell migration as well [27, 28].

Initially Eph/ephrin signaling was believed to be an intrinsically repulsive guidance mechanism, but this simple story was soon complicated by the discovery [29] that Eph/ephrin differences uniquely mark arteries and veins, prior to morphological differentiation, and that the function of ephrin proteins is required for formation of the cardiovascular system. Mice lacking these genes suffer profound defects in angiogenesis and cardiovascular development [30-32]. Additional complications emerged as it became clear that ephrin signaling is not obligately repulsive, but instead can mediate adhesive interactions as well [33], possibly through the use of different splice variants of the Eph receptor [34]. Recent efforts demonstrated that the cytoplasmic domains of ephrin-B2 as critical for arterial development, but dispensable for cranial neural crest migration [35]. Finally, progress has also been made in working out various aspects of signal transduction downstream of both Eph and ephrin [36] [[37].

Cell Migration Assays

Central Logic of Our Experiments

There were two guiding principles in our design of a cell migration assay. We wanted to evaluate cellular responses to a choice between two substrates, not control cell behavior. The second was that we sought to improve the technical underpinnings of the stripe assay in order to remove extraneous sources of non-

biological variability (e.g., systematic patterning artifacts) so that we could quantitatively measure both the normal response of neural crest cells to ephrin-B ligands and the normal degree of variability in that response. By carefully controlling the presentation of ephrin-B guidance cues to neural crest cells, we sought to standardize the experimental design sufficiently that different neural crest cells would be presented with the same migration choice. By visualizing and measuring those responses using time-lapse microscopy, we expected that we could catalog the range of possible responses and that we would eventually be able to predict what a given cell should do in response to a given experimental setup, Once we knew what that reaction was, so long as it was predictable, we then planned to study the signal transduction requirements for that response via pharmaceutical inhibition of various cellular pathways, starting with transcription and translation.

We based our approach loosely on an assay known as the “stripe assay,” which has been used to test the involvement of specific molecules on axon guidance and neural crest migration behavior [1, 24, 27]. In this assay, candidate molecules are physically adsorbed in patterns onto nitrocellulose-coated tissue culture plastic. Cells are then cultured on these patterned surfaces, and candidate molecules are scored based on the degree to which cells have accumulated on the stripes at some later time (Figure 2-1). If more cells avoid the stripes than occupy them, the candidate molecule is classified as a repulsive agent. If there is no obvious pattern, then the molecule is judged to be

permissive. Some efforts have been made to extend this analysis by filming the cells, using time-lapse microscopy, as they are migrating [2]. However, these efforts are greatly hindered by the intrinsic unsuitability of the classic stripe assay for high-resolution microscopy.

The problems are not intrinsic in the conceptual design of the assay, but rather in the experimental implementation. The first problem is that patterns are defined by a physical grid of flow channels, which is pressed into nitrocellulose coated plastic. This approach severely limits pattern design to those which are amenable to flow channels. Additionally, cells are sensitive to very small differences in surface topology [38, 39]; consistent with this concern, a recent research article utilizing the stripe assay reported a tendency of cells to non-specifically avoid the stripe that is laid down first, independent of protein content [40]. Furthermore, since the deposition relies on non-specific adsorption, it is difficult to produce highly uniform regions; inevitably there are regions of high and low protein adsorption even in identically treated areas. Finally, both the plastic tissue culture dish and the nitrocellulose used to coat the dish directly hinder high-resolution imaging. Plastic is autofluorescent and scatters light, while the nitrocellulose leaves cell sized artifacts throughout the field of view. We sought to address both of these deficiencies by developing a more robust patterning chemistry on thin glass coverslips.

Materials and Methods/Experimental Techniques

Time-Lapse Imaging

Time-lapse movies were collected on a Zeiss 410 confocal laser scanning microscope (CLSM) or a Zeiss Pascal CLSM. For imaging neural crest cultures, the CLSM were outfitted with a temperature controlled chamber which maintains a constant 37° C.

Neural crest cells display extensive protrusive activity in culture. In order to temporally resolved the membrane and cytoskeletal dynamics of neural crest cell migration, it proved necessary to acquire images every 1-20 seconds. Conversely we needed to follow these cells for minutes to hours in order to determine their reaction to the substrate patterns. This balance of frequent imaging over long time periods required that we be very careful not to damage the cells with excessive light exposure. When we began this project we could image actin-GFP in neural crest cells at very high resolution, but the signal would fade very rapidly. To successfully image such dim fluorescent labels, three elements were critical: careful choice of objective lenses, custom designed filters and dichroics, and careful management of light exposure.

The brightness of an image on a standard confocal microscope scales with the fourth power of the numerical aperture (NA) of the objective lens. The numerical aperture captures both the geometry of the lens and the optical properties of the immersion media between the lens and the sample. Due to this steep

dependence of brightness on NA, small changes in the NA have very large effects on the collected image, as demonstrated in Figure 2-1. We tested the full range of Zeiss objective lenses for imaging and found the 20x Fluar, 40x C-Apochromat, and 63x Plan-Apochromat to provide superior performance for our applications.

The second change that we made to the Zeiss 410 was to upgrade all of the emission filters and dichroic mirrors with custom optics from Chroma Corporation (Brattleboro, VT). In collaboration with Michael Stanley of Chroma Corporation we optimized the internal optics of the 410 for imaging green fluorescent protein. We conducted tests on the efficiency of the system before and after the upgrade and observed a tenfold increase in sensitivity on the green channel, as illustrated in Figure 2-2.

The single most important factor for successful imaging of dim fluorescent labels in living samples is the careful management of the excitation light power levels. It is typically possible to generate equivalent quality images of the same sample over incident power levels that vary by at least tenfold. There is no obvious signal from the microscope or the image that one could get equivalent results with less light. To accommodate this fact, we generally started imaging with very significant (100-300 fold) attenuation of the incident laser intensity, and only slowly increased the laser power until a reasonable image was achieved. This approach was critical to our fluorescent imaging, as we empirically noted a

threshold effect in our samples, whereby the cells could tolerate a certain amount of light without photobleaching or obvious photodamage. However once that threshold was exceeded the damage could be swift and irreparable. The effect of incident light power on image quality and photobleaching is demonstrated in Figure 2-3.

Imaging Chambers

Prior *in vitro* culture of neural tube explants in the Fraser Lab had been performed in standard 35 mm plastic tissue culture dishes [2]. These chambers were inexpensive and convenient, but the thick plastic bottom was incompatible with differential interference contrast microscopy and was too thick to allow access for high NA objective lenses. To overcome these difficulties we tested several alternative imaging chambers, illustrated in Figure 2-4. There were three basic variants, the porthole chamber, the o-ring chamber, and the chambered coverslip. Porthole chambers were convenient and inexpensive to prepare in large numbers. Four well multidishes (Nunc Nunclon Delta 176740) or 35 mm tissue culture dishes (Falcon 35-3001) were modified in the Chemistry Machine Shop at Caltech, by removing a 15-17 mm circle from the bottom surface of each of the wells. We then attach a patterned glass substrate to the bottom surface of the culture well using silicon grease. By replacing portions of the lids of these chambers with glass, we are able to create an all glass optical path, thereby allowing differential interference contrast (DIC) microscopy methods. These chambers have worked well for imaging and can be reused by cleaning and sterilizing with 70% ethanol and hard UV between uses. The four well chambers

allowed us to use smaller amounts of media and protein reagents. When combined with a programmable moveable microscope stage, these multiwell imaging chambers allow us to simultaneously image several neural crest cultures.

Alternate designs included an o-ring chamber (pictured in Figure 2-4B) that was made by Herb Adams at Caltech's Central Plant. This chamber is very similar to the Attofluor cell chamber (Molecular Probes, A-7816), except that the top of the chamber is made of Delrin instead of stainless steel. We substituted Delrin for stainless steel for all surfaces in contact with cells, because an all stainless steel cell culture chamber was tested and found to be acutely toxic to neurons and neural crest cells (though not to NIH/Swiss 3T3 fibroblasts). This highlights the importance of careful selection of materials for cell culture, and the importance of testing a chamber with the actual cells of interest. With the Delrin top it was compatible with neural crest cell cultures and was convenient to load, but it was difficult to maintain sterile cultures in the chamber and so it was not used frequently. Another convenient commercially available option was the Nalge/Nunc Lab-Tek chamber (Figure 2-4C), which consisted of plastic culture chambers bonded to either coverslips or slides. Though more fragile, the coverglass chambers were more useful as the slide chambers were too thick for the working distance of high performance microscope objectives. These were the chambers of choice when working with cells, such as fibroblasts, that readily

adhere to bare glass (as in the mouse embryo fibroblasts used in the paper described in Appendix 1), but were not as useful with neural crest cells.

Labeling Neural Crest Cells In Vitro and In Vivo

In order to specifically highlight different subcellular components of migrating neural crest cells, I tested a range of different green fluorescent protein (GFP) fusion proteins. In a separate, but synergistic research effort within the Fraser Lab, Rusty Lansford has been developing a set of retroviruses to deliver proteins to avian cells. He generated replication-defective VSV-G pseudotyped retroviral viruses that express GFP or LacZ marker to infect avian embryos [41]. Pseudotyping alters the host range of a virus by exchanging the surface antigens among both DNA and RNA viruses [42]. The resulting VSV-G pseudotyped retroviruses possess a broad host range and can be concentrated 1000-fold with minimal loss of biological activity These viruses are capable of infecting nearly any cell in the avian embryo, including neural crest cells, and do not appear to negatively affect cellular development. I tested a large number of these viral constructs in avian embryos. The most useful were viruses that delivered a nuclear GFP (Clontech Histone2B EGFP), mitochondrial YFP (Clontech EYFP-Mito 632347), membrane GFP (Clontech Gap43-EGFP), or actin GFP (Clontech EGFP-Actin 632348). The GFP fusion proteins express well in avian cells and I have successfully imaged each of them for extended durations in living cells using confocal microscopy.

The major advantage of these labels was that they are readily applied to cultured neural crest cells or injected into neural tubes *in situ*, they are cell permanent, and they integrate stably into the target cell's genome, providing a faithful lineage label. The drawback is that there is a typical delay of 18-24 hours between infection and expression.

Neural Crest Explant Cultures

To enable us to study neural crest cell migration in the simplest possible context, we cultured isolated neural tubes *in vitro*. Neural tube explants can be maintained in culture for days, and each neural tube can produce hundreds of neural crest cells. Trunk neural crest explants were performed in general accordance with standard methods [43], with several variations. When I first joined the lab it was common to allow neural tubes to adhere to the substrate in a minimal volume of media for 45 minutes prior to adding the full amount of media to the culture dish. This protocol gave unpredictable results and I tested simply adding the neural tubes to the bottom of a dish full of media and found that it worked well with all substrates.

Additionally, when I joined the lab the standard neural crest culture medium was Dulbecco's Modified Eagle's Medium (DMEM) with 10% chick embryo extract, 15% horse serum, 1% penicillin/streptomycin, 1% non-essential amino acids, and 1% L-glutamine. This is a very rich medium containing an unknown number of stimulatory proteins. After consulting with Martin Garcia-Castro, I tested a serum-free media and a chemically defined media and had good results with

both. The serum free media produced equally robust cultures as the serum containing media. The chemically defined media was only suitable for short term culture. Full details of the media formulations, suppliers, and a detailed protocol for neural tube explant cultures are presented in Appendix 2.

One final improvement on the neural tube explant protocol was that I noticed that cultures changed dramatically after 24 hours if the neural tube was allowed to remain with the neural crest cells. The cells grew into a dense monolayer and did not interact much with substrate patterns. When the neural tube was removed at 6 hours after explanting the neural crest cells maintained a disperse arrangement, and removal after 15.5 hours produced an intermediate arrangement. For details see Figure 2-7. Recombinant ephrin-B1 for migration experiments was initially acquired through a generous gift from Regeneron Corporation to Rusty Lansford. Subsequent stocks were commercially acquired from R&D Systems (473-EB-200). In both cases ephrin-B1 was fused to the FC domain.

Traditional Adsorption Based Stripe Assays

Patterns of proteins were prepared on plastic and glass substrates via non-specific adsorption of protein through flow channels in silicone molds (acquired from Juergen Jung, MPI f. Entwicklungsbiologie). These were done in accordance with published protocols. Appendix 2 presents a detailed protocol for this method.

As an alternative I tried generating patterns of proteins by adsorbing proteins to vacuum deposited chlorosilane monolayers on glass, after consultations with Chris Chen and Sri Rhagavan of Johns Hopkins University. The protocol I used is in Appendix 2 and representative good and bad patterns are presented in Figure 2-15. Eventually, I concluded that it was not possible to push the analysis of neural crest response to ephrin-B signaling further with adsorbed stripe patterns and focused exclusively on photolithographically produced patterned substrates.

A New Method to Produce Patterned Substrates

We wanted to design an experimentally convenient, cost effective, additive patterning technique capable of patterning proteins on glass surfaces with 2-10 micron resolution. It was also critical that the final product be compatible with culturing primary neural crest cells. We believe our current assay system satisfies all of these criteria.

A schematic overview of our approach is presented in Figure 2. We begin with glass coverslips, acid wash them, then coat them in a self assembled layer of aminopropyltriethoxy-silane (APTES). Self assembled layers of this type have several advantages. First, the reagents are cheap and the layers are experimentally easy to prepare. Second, their lateral organization is largely independent of the terminal group (in this case a primary amine), so that we can subsequently derivatize the surface with crosslinkers and proteins without unduly

disrupting the structure of the silane layer [44]. We designed the system to covalently link the proteins to the surface, as previous studies had demonstrated that antibody activity on a surface was preserved for longer if the antibody was covalently immobilized, rather than adsorbed [45]. For these studies, we have used a commercially available photoactivatible cross-linker, 4-benzoylbenzoic acid succinimidyl ester (Molecular Probes B-1577).

At the time we began these studies, there was intense interest binding proteins to surfaces to generate biosensors of various kinds. Many of these approaches relied on photopatterning, as conventional microchip patterning technology is already based on photolithography (reviewed in [46]). Several papers were of particular use as we developed our own protocols [47-49].

Two different protocols that we developed for generating photolithographic patterns of proteins on glass are presented in Appendix 2. The main protocol was optimized to make use of only ethanol and dimethylsulfoxide as organic solvents. This optimization proved critical for maintaining viable primary cultures on the coverslips. An older protocol is also presented in Appendix 2 for comparison.

Many of the published methods of generating patterned protein surfaces used a destructive patterning technique (i.e., hard X-ray irradiation) to render some portion of the surface incompatible with protein binding. We were concerned that

patterns of this type would also make those regions less compatible with cellular migration, thereby biasing our assay. For this reason, we make uniform layers of a photoactivatible molecule, then use light to add our test protein in a pattern, and a migration permissive molecule (i.e., fibronectin) uniformly on the surface. Our method yields patterned substrates which structurally differ only in the amount and type of protein immobilized, the surface structure of the layer does not change.

Selection of Photoactivatible Group

We chose to work with a benzophenone based cross-linker, because benzophenone functional groups can be repeatedly excited at their excitation maximum. Many of the other commonly available photoreactive groups will bind to a solvent molecule if no protein is around. Under those circumstances all work would be done under a red safe light [50]. The bifunctional crosslinker reacts chemically with the primary amine of the APTES layer in neat DMSO, forming a uniform layer of photoreactive molecules, as assayed by the distribution of bound fluorescent molecules. The photoreactive benzophenone functionality of the crosslinker was chosen chiefly because it has an activation peak at about 350 nm, which should not damage proteins [50, 51]. This particular cross-linker was well suited to our current needs.

Photolithography

The photolithography is carried out in Michael Roukes' physics lab on a standard mask aligner. The mask aligner provides us with a convenient way of positioning our sample coverslip in close proximity to the lithographic mask. The derivatized coverslip is coated in a small volume (30-100 microliters over ~5 square centimeters) of concentrated protein solution (generally ~1 mg/mL) and positioned using the mask aligner's stage. The stage has micrometer controls that allow translation in all three dimensions, as well as rotation in the plane, to allow the coverslip to be brought into close proximity to the patterned mask.

Once the coverslip is positioned, the sample is exposed to fluorescent light from a highly uniform mercury arc lamp (<10% intensity variation over the width of the 3 inch sample stage). We have found empirically that exposures at a luminescence of 10 mW/cm^2, for between 2 and 10 minutes give steadily increasing concentrations of bound protein, as assayed by the fluorescence of immobilized fluorescein tagged proteins. After exposure, the coverslips are rinsed in phosphate buffered saline (PBS) several times and are then ready for use. To get patterns of multiple proteins, you can use several exposures, though in practice we never achieved more than two.

A major technical challenge for getting the patterned substrates to work as a migration assay is how to provide a uniformly permissive surface, with no differences in levels of adhesiveness. Neural crest cells require extracellular

matrix proteins to migrate and we used fibronectin to support migration. Initially we added fibronectin to the photolithography solution and attached it to the surface at the same time as the ephrin, then followed up with solution adsorption of fibronectin everywhere. We became concerned that this could be convoluting an adhesive difference in with the ephrin difference though, so in most of our experiments ephrin was immobilized with a fluorescent bovine serum albumin (to visualize the pattern), then the whole coverslip was soaked in 10 ug/mL human fibronectin (BD Labware).

Results

Improved Vital Labels

We developed labeling and imaging protocols to specifically label the nucleus, mitochondria, actin cytoskeleton, and plasma membrane of migrating primary neural crest cells. Figure 2-6 contains representative images of the four best GFP fusion proteins we test. These GFP fusions fall into two of major classes based on their role in our experiments: cellular markers and cytoskeletal labels.

The nuclear, mitochondrial, and plasma membrane fusions are excellent markers for tracking the positions of migrating cells. The nuclear localized GFP is a fusion of histone 2B with EGFP (H2B-EGFP) and provides a very bright concentrated signal that was extremely useful for following the trajectories of many cells which are closely spaced. It serves as a direct substitute in our

experiments for more traditional dyes such as DiI or rhodamine dextran, since H2B-EGFP is brighter, bleaches less quickly, doesn't dilute with cell divisions, and provides a more easily tracked geometry. The plasma membrane fusion is a short membrane localization sequence (~30 amino acids) from the GAP-43 protein fused to EGFP. It is an excellent marker for membrane movements, filopodia, and membrane ruffles in relatively disperse cell populations, such as neural crest cells migrating on coverslips at low density. The mitochondrial label is a fusion of a mitochondrial targeting sequence with EYFP. It is a very interesting marker for double labeling experiments as its distinct localization allows its presence to be verified, even when coexpressed with other EYFP fusion proteins. Coincidentally, test movies of neural crest cells labeled with mito-EYFP led directly to the collaboration described in Appendix 1.

Three other GFP fusions allowed us to image the cytoskeleton in living neural crest cells. We tested fusions of EGFP, EYFP, and ECFP to human beta-actin, human alpha-tubulin, and tau (a microtubule binding protein). We have infected neural crest cells with retroviruses containing each of these three proteins. Morphologically the neural crest cells appear to be normal. Of the three, the actin GFP proved most useful as it gave us the most specific cytoskeletal staining with the least cytoplasmic background.

Photolithography of Biological Macromolecules

Our photolithographic method of producing patterned substrates reliably produced patterned substrates. Improvements over the old style “stripe assay” include improved optical clarity, covalent protein tethering, and much greater uniformity and fidelity in our patterns. Since the pattern was imposed by light, rather than fluid flow, we were able to design the pattern to match the experiment, rather than the reverse. Sample patterns, visualized by immobilizing fluorescently tagged proteins, are presented below to give an idea of the current resolution and uniformity of our system (Figure 2-10B). We have immobilized streptavidin, bovine serum albumin, various antibodies, ephrin-B1, and fibronectin. For contrast, we also show a representative image of fluorescently tagged protein prepared using the standard adsorption approach (Figure 2-10A).

Furthermore, we have tested these substrates for toxicity and all current data shows that they are highly supportive of neural crest cell outgrowth, migration, proliferation, and differentiation. Patterned substrates were not initially compatible with primary neural crest cell cultures and Appendix 2 presents a solvent optimized protocol (A2-2) and an earlier protocol (A2-4) that gave good patterns but left some type of residue that was toxic to neural crest cells. Cultures explanted on substrates prepared with protocol A2-2 were indistinguishable in health and morphology from cultures prepared on plastic. Thus, we believe that we have generated a suitable substrate for testing the effects of candidate guidance cues on neural crest cell migration.

Traditional "Stripe Assays"

To provide a baseline for comparison with previous work, I repeated the stripe assays with ephrin-B1 stripes on a background of fibronectin according to published protocols [2]. My findings generally confirmed the results of that paper, in that cells seemed to generally avoid the ephrin-B1 areas, but the response was somewhat variable. The full range of responses are presented in Figure 2-11. A close examination of one of those time-lapse movies (Figure 2-12) reveals that though several of the neural crest cells appear confined by the adsorbed stripes of ephrin-B1 (notably the cell indicated with the small white arrow), other cells (large white arrow), do not respect the stripe boundaries and migrate over them.

One confounding variable that was addressed was that cultures became less reactive to the substrates over time, possibly due to cell differentiation within the cultures, and so I focused my imaging efforts on the first 12-24 hours after explanting, while the cells were first encountering the patterns. This precluded labeling the neural crest cells with viruses, unless the virus was injected into very early embryos first, and so I began imaging with differential interference contrast microscopy.

Photolithographic Stripe Assays

We used our new photolithographed substrates to evaluate the effects of ephrin-B1 on neural crest migration. Figure 2-13 presents representative still images from time-lapse movies of neural crest cultures on substrates where ephrin-B1 was laid down in stripes against a uniform background of fibronectin. For clarity of presentation, the bright field image was overlaid with traces of where the stripes were. In each case presented here there were fewer cells in the ephrin-B1 regions, but this was not universally true in all dishes or all experiments.

Our observations agreed generally with results obtained from the previous patterning method [2]; neural crest cells could migrate onto regions containing ephrin-B1, but they would subsequently undergo an ephrin mediated collapse, pull off the ephrin-B1 region and undergo extensive membrane ruffling. The montage in Figure 2-14 captures a retraction event: we can see that the neural crest cell has migrated into an ephrin-B1 domain, and that it actively explores its environment with multiple lamellapodia. We can also see that the cell retracts its entire cell body onto a permissive region and blebs for several minutes.

In the montage series on glass, we can see clearly that the retraction is not a single event, but rather three sequential retractions. It is very interesting to note that in the final frame, even though the neural crest cell is nearly completely collapsed, the cell maintains very fine connections to the ephrin-B1 containing region it just left, indicating that the cell collapses its lamellapodia, but leaves

retraction fibers. The fact that the crest cell maintains connections to the ephrin-B1 surface, even during the collapse, strongly implies that the ephrin-B1 region is adequate for neural crest adhesion, and that the collapse is due to a signaling event, not a lack of mechanical traction and is consistent with growth cone behavior in response to other guidance cues [52]. Another interesting detail that emerges from the new series is that the lamellapodia do not simply pull back: the uppermost lamillapod clearly sends a “pulse” of membrane up towards its distal end. Only after this pulse does the lamellapod collapse.

Though this frame by frame analysis is compelling, it would not be accurate to characterize it as typical. It was typical of one category of cellular response to ephrin-B1 patterns, but other categories existed. Some cells seemed more mildly repulsed by ephrin-B1 regions, many more seemed to ignore them entirely, and in a rare experiment or two neural crest cells accumulated preferentially on regions that should have contained more ephrin-B1. We successfully achieved greater experimental control over the patterning, culture, and imaging methods, but this increased experimental control did not effectively reduce the variability in the observed cellular response.

Discussion

Previously, repulsive cues for neural crest cell migration were defined by the relative abundance of cells on patterned substrates [1, 2]. We designed an improved migration assay to standardize the experimental conditions in the expectation that this improved experimental control would result in more

consistent cellular responses. We then planned to use this consistent cellular response (whatever it turned out to be), as the normal cell behavior and attempt to work out the subcellular processes required to generate this behavior. The key requirement of our assay was cellular predictability; the cell's response to our imposed migration choice needed to be reasonably consistent from cell to cell and day to day.

I was very consciously modeling my efforts on the growth cone turning assay, in which small amounts of soluble molecules were introduced into a culture dish near a pathfinding growth cone. Certain molecules (e.g., netrin) cause growth cones to reliably turn towards or away from the stimulus. By interfering with cellular signaling pathways and then observing the resulting effect on the expected turning response, great progress has recently been made in determining downstream molecular players in these signal transduction cascades [53-57].

In our case there was a long list of desired improvements to the assay: optically better culture chambers, improved specific contrast, cell culture in serum free media, improved patterning methods, cell culture compatibility with the improved substrates, and cellular interaction with the imposed patterns. All of these individual features were achieved and several were dramatic successes. What I failed to sufficiently appreciate early in graduate school was that all of these were contingent successes, contingent on the nature of the final cellular response to

these patterns. If the cells reacted consistently to the patterns, then we could do, as planned, signal transduction experiments and work out the cellular requirements for ephrin-B1 signaling. Unfortunately improved experimental control did not bring appreciably improved cellular predictability. We could only conclude, as was already known, that neural crest cells appear repulsed by ephrin-B1.

When we began these experiments, ephrin-B ligands were known to be a repulsive guidance molecule for neural crest cells *in vitro*, but there was significant variability in the response of individual cells to patterns of ephrin-B. By improving the technical implementation of the assay we sought to test whether we were observing a constant response to a variable signal (e.g., variations in the substrate pattern) or a variable response to a constant signal. Since we made the cell culture and the patterning significantly more consistent and observed no reduction in the variability we concluded that the variation was inherent in the neural crest cells themselves.

Connection to Chapter 3

One interpretation that we did take away from these experiments was that the stripe assay was intrinsically unsuited to determining the timing and events of the early cell behavioral response to ephrin-B1 signaling in neural crest cells, as it was difficult to reliably image a cell's first contact with the ephrin-B1 substrate. The one aspect of the stripe assay that I became dissatisfied with was that each

cell experienced the pattern differently. Some migrated out onto the stripe pattern directly and others likely never saw it. The control over the time course of the assay was left up to the cell and to chance. I wanted a greater ability to control the presentation of the ligand exposure directly. To address this lingering variability, and create a greater uniformity of cellular experience within the assay, I designed another migration assay, described in Chapter 3, to specifically address test the timing and typical response of migrating primary neural crest cells to focal ephrin-B stimulus.

1. Wang HU, Anderson DJ: **Eph family transmembrane ligands can mediate repulsive guidance of trunk neural crest migration and motor axon outgrowth**. *Neuron* 1997, **18**:383-396.
2. Krull CE, Lansford R, Gale NW, Collazo A, Marcelle C, Yancopoulos GD, Fraser SE, Bronner-Fraser M: **Interactions of Eph-related receptors and ligands confer rostrocaudal pattern to trunk neural crest migration**. *Curr Biol* 1997, **7**:571-580.
3. Baker CV, Bronner-Fraser M: **The origins of the neural crest. Part I: embryonic induction**. *Mech Dev* 1997, **69**:3-11.
4. Bronner-Fraser M: **Origins and developmental potential of the neural crest**. *Exp Cell Res* 1995, **218**:405-417.
5. Anderson DJ: **Genes, lineages and the neural crest: a speculative review**. *Philos Trans R Soc Lond B Biol Sci* 2000, **355**:953-964.
6. Hall B: *The Neural Crest in Development and Evolution*, 1st edn. New York: Springer; 1999.
7. Le Douarin N, Kalcheim C: *The Neural Crest*, 2nd edn. Cambridge: Cambridge University Press; 1999.
8. Bronner-Fraser M, Fraser S: **Developmental potential of avian trunk neural crest cells in situ**. *Neuron* 1989, **3**:755-766.
9. Fraser SE, Bronner-Fraser M: **Migrating neural crest cells in the trunk of the avian embryo are multipotent**. *Development* 1991, **112**:913-920.
10. Bronner-Fraser M, Stern C: **Effects of mesodermal tissues on avian neural crest cell migration**. *Dev Biol* 1991, **143**:213-217.
11. Perris R: **The extracellular matrix in neural crest-cell migration**. *Trends Neurosci* 1997, **20**:23-31.
12. Henderson DJ, Copp AJ: **Role of the extracellular matrix in neural crest cell migration**. *J Anat* 1997, **191 (Pt 4)**:507-515.
13. Landolt RM, Vaughan L, Winterhalter KH, Zimmermann DR: **Versican is selectively expressed in embryonic tissues that act as barriers to neural crest cell migration and axon outgrowth**. *Development* 1995, **121**:2303-2312.
14. Nakagawa S, Takeichi M: **Neural crest emigration from the neural tube depends on regulated cadherin expression**. *Development* 1998, **125**:2963-2971.
15. Liu JP, Jessell TM: **A role for rhoB in the delamination of neural crest cells from the dorsal neural tube**. *Development* 1998, **125**:5055-5067.
16. Debby-Brafman A, Burstyn-Cohen T, Klar A, Kalcheim C: **F-Spondin, expressed in somite regions avoided by neural crest cells, mediates inhibition of distinct somite domains to neural crest migration**. *Neuron* 1999, **22**:475-488.
17. Eickholt BJ, Mackenzie SL, Graham A, Walsh FS, Doherty P: **Evidence for collapsin-1 functioning in the control of neural crest migration in both trunk and hindbrain regions**. *Development* 1999, **126**:2181-2189.

18. Cai DH, Brauer PR: **Synthetic matrix metalloproteinase inhibitor decreases early cardiac neural crest migration in chicken embryos**. *Dev Dyn* 2002, **224**:441-449.
19. Krull CE, Collazo A, Fraser SE, Bronner-Fraser M: **Segmental migration of trunk neural crest: time-lapse analysis reveals a role for PNA-binding molecules**. *Development* 1995, **121**:3733-3743.
20. Drescher U, Bonhoeffer F, Muller BK: **The Eph family in retinal axon guidance**. *Curr Opin Neurobiol* 1997, **7**:75-80.
21. Mellitzer G, Xu Q, Wilkinson DG: **Control of cell behaviour by signalling through Eph receptors and ephrins**. *Curr Opin Neurobiol* 2000, **10**:400-408.
22. Orioli D, Klein R: **The Eph receptor family: axonal guidance by contact repulsion**. *Trends Genet* 1997, **13**:354-359.
23. Xu Q, Mellitzer G, Wilkinson DG: **Roles of Eph receptors and ephrins in segmental patterning**. *Philos Trans R Soc Lond B Biol Sci* 2000, **355**:993-1002.
24. Drescher U, Kremoser C, Handwerker C, Loschinger J, Noda M, Bonhoeffer F: **In vitro guidance of retinal ganglion cell axons by RAGS, a 25 kDa tectal protein related to ligands for Eph receptor tyrosine kinases**. *Cell* 1995, **82**:359-370.
25. Walter J, Kern-Veits B, Huf J, Stolze B, Bonhoeffer F: **Recognition of position-specific properties of tectal cell membranes by retinal axons in vitro**. *Development* 1987, **101**:685-696.
26. Santiago A, Erickson CA: **Ephrin-B ligands play a dual role in the control of neural crest cell migration**. *Development* 2002, **129**:3621-3632.
27. Smith A, Robinson V, Patel K, Wilkinson DG: **The EphA4 and EphB1 receptor tyrosine kinases and ephrin-B2 ligand regulate targeted migration of branchial neural crest cells**. *Curr Biol* 1997, **7**:561-570.
28. Helbling PM, Tran CT, Brandli AW: **Requirement for EphA receptor signaling in the segregation of Xenopus third and fourth arch neural crest cells**. *Mech Dev* 1998, **78**:63-79.
29. Wang HU, Chen ZF, Anderson DJ: **Molecular distinction and angiogenic interaction between embryonic arteries and veins revealed by ephrin-B2 and its receptor Eph-B4**. *Cell* 1998, **93**:741-753.
30. Adams RH, Wilkinson GA, Weiss C, Diella F, Gale NW, Deutsch U, Risau W, Klein R: **Roles of ephrinB ligands and EphB receptors in cardiovascular development: demarcation of arterial/venous domains, vascular morphogenesis, and sprouting angiogenesis**. *Genes Dev* 1999, **13**:295-306.
31. Gerety SS, Anderson DJ: **Cardiovascular ephrinB2 function is essential for embryonic angiogenesis**. *Development* 2002, **129**:1397-1410.
32. Gerety SS, Wang HU, Chen ZF, Anderson DJ: **Symmetrical mutant phenotypes of the receptor EphB4 and its specific transmembrane**

ligand ephrin-B2 in cardiovascular development. *Mol Cell* 1999, **4**:403-414.

33. Huynh-Do U, Vindis C, Liu H, Cerretti DP, McGrew JT, Enriquez M, Chen J, Daniel TO: **Ephrin-B1 transduces signals to activate integrin-mediated migration, attachment and angiogenesis**. *J Cell Sci* 2002, **115**:3073-3081.
34. Holmberg J, Clarke DL, Frisen J: **Regulation of repulsion versus adhesion by different splice forms of an Eph receptor**. *Nature* 2000, **408**:203-206.
35. Adams RH, Diella F, Hennig S, Helmbacher F, Deutsch U, Klein R: **The cytoplasmic domain of the ligand ephrinB2 is required for vascular morphogenesis but not cranial neural crest migration**. *Cell* 2001, **104**:57-69.
36. Cowan CA, Henkemeyer M: **The SH2/SH3 adaptor Grb4 transduces B-ephrin reverse signals**. *Nature* 2001, **413**:174-179.
37. Wahl S, Barth H, Ciossek T, Aktories K, Mueller BK: **Ephrin-A5 induces collapse of growth cones by activating Rho and Rho kinase**. *J Cell Biol* 2000, **149**:263-270.
38. Brunette DM: **Effects of Surface Topography of Implant Materials on Cell Behavior in vitro and in vivo**. In: *Nanofabrication and Biosystems* Edited by Hoch HC, Jelinski LW, Craighead HG. pp. 423. Cambridge: Cambridge University Press; 1996: 423.
39. Clark P: **Cell and Neuron Growth Cone Behavior on Micropatterned Surfaces**. In: *Nanofabrication and Biosystems* Edited by Hoch HC, Jelinski LW, Craighead HG. pp. 423. Cambridge: Cambridge University Press; 1996: 423.
40. Hornberger MR, Dutting D, Ciossek T, Yamada T, Handwerker C, Lang S, Weth F, Huf J, Wessel R, Logan C, Tanaka H, Drescher U: **Modulation of EphA receptor function by coexpressed ephrinA ligands on retinal ganglion cell axons**. *Neuron* 1999, **22**:731-742.
41. Okada A, Lansford R, Weimann JM, Fraser SE, McConnell SK: **Imaging cells in the developing nervous system with retrovirus expressing modified green fluorescent protein**. *Exp Neurol* 1999, **156**:394-406.
42. Zavada J: **The Psuedotypic Paradox**. *J Gen Virol* 1982, **63**:15-24.
43. Bronner-Fraser M: **Manipulations of Neural Crest Cells or Their Migratory Pathways**. In: *Methods in Avian Embryology* Edited by Bronner-Fraser M, vol. 51. pp. 61-79. New York: Academic Press; 1996: 61-79.
44. Arkles B: **Silane Coupling Agent Chemistry**. In: *Silicon Compounds: Register and Review* Edited by Technologies UC, 5th ed. pp. 301. Bristol: United Chemical Technologies; 1996: 301.
45. OrtegaVinuesa JL, BastosGonzalez D, HidalgoAlvarez R: **Effect of storage time on the immunoreactivity of IgG physically adsorbed or chemically bound to latex beads**. *Journal of Colloid and Interface Science* 1996, **184**:331-334.

46. Sigrist H, Collioud A, Clemence JF, Gao H, Luginbuhl R, Sanger M, Sundarababu G: **Surface Immobilization of Biomolecules by Light**. *Optical Engineering* 1995, **34**:2339-2348.
47. Sigrist H, Gao H, Wegmuller B: **Light-Dependent, Covalent Immobilization of Biomolecules on Inert Surfaces**. *Bio-Technology* 1992, **10**:1026-1028.
48. Sanger M, Sigrist H: **Light-dependent immobilization of biomolecules on material and lipid bilayer membrane surfaces**. *Sensors and Actuators a-Physical* 1995, **51**:83-88.
49. Rozsnyai LF, Benson DR, Fodor SPA, Schultz PG: **Photolithographic Immobilization of Biopolymers on Solid Supports**. *Angewandte Chemie-International Edition in English* 1992, **31**:759-761.
50. Dorman G, Prestwich G: **Benzophenone Photophores in Biochemistry**. *Biochemistry* 1994, **33**:5661-5673.
51. Prestwich G, Dorman G, Elliot J, Marecak D, Chaudhary A: **Benzophenone Photoprobes for Phosphoinositides, Peptides, and Drugs**. *Photochemistry and Photobiology* 1997, **65**:222-234.
52. Raper JA, Grunewald EB: **Temporal retinal growth cones collapse on contact with nasal retinal axons**. *Exp Neurol* 1990, **109**:70-74.
53. Timothy M. Gomez ER, Mu-ming Poo, Nicholas C. Spitzer: **Filopodial Calcium Transients Promote Substrate-Dependent Growth Cone Turning**. *Science* 2001, **291**:1983-1987.
54. Hopker VH, Shewan D, Tessier-Lavigne M, Poo M, Holt C: **Growth-cone attraction to netrin-1 is converted to repulsion by laminin-1**. *Nature* 1999, **401**:69-73.
55. Song H, Ming G, He Z, Lehmann M, McKerracher L, Tessier-Lavigne M, Poo M: **Conversion of neuronal growth cone responses from repulsion to attraction by cyclic nucleotides**. *Science* 1998, **281**:1515-1518.
56. Ming GL, Song HJ, Berninger B, Holt CE, Tessier-Lavigne M, Poo MM: **cAMP-dependent growth cone guidance by netrin-1**. *Neuron* 1997, **19**:1225-1235.
57. Ming GL, Wong ST, Henley J, Yuan XB, Song HJ, Spitzer NC, Poo MM: **Adaptation in the chemotactic guidance of nerve growth cones**. *Nature* 2002, **417**:411-418.

Figure 2-1: A schematic view of the conceptual design of the stripe assay. Alternating stripes of a potential guidance molecule (gray) are overlaid on a uniformly permissive background (white). The neural tube (blue) is then explanted onto the surface. If the cells accumulate uniformly the test molecule is classified as permissive. If the accumulate preferentially on the white areas, the test molecule is classified as repulsive.

Figure 2-2: A comparison of the relative brightness of images collected by different objective lenses. All images are collected on a Zeiss Pascal confocal laser scanning microscope, of Bodipy Fl phallacidin stained bovine pulmonary artery endothelial cells (Molecular Probes, FluoCells #1, F-14780). Each pair of images (A-B and C-D) were collected with the same imaging parameters; the only difference between the two images is in the objective lens. It is worth noting that the higher numerical aperture (NA) lens will generate a brighter image both because it delivers light more efficiently and because it collects the light more efficiently.

Figure 2-3: Panel A depicts the portion of the emission spectrum of GFP which is accessible to a typical filter and dichroic combination. As much as half of the emission spectra does not even arrive at the detector, as it is not efficiently transmitted through the intermediate optics. Panel B shows that the redesigned filters that we generated (Chroma Corporation, primary dichroic q497lp and emission filter HQ500lp) transmit a greater fraction of the emission spectra of

GFP, resulting in increased collection efficiency. These savings can be used to generate a higher quality image with the same amount of light, or to generate an equivalent quality image with less intense light or in a shorter period of time. Panel C shows the quality of images of actin-GFP labeled fibroblasts that we were able to generate with a Zeiss NT 488/568 primary dichroic and a LP515 emission filter. Panel D shows the quality of images that we collected, of a different region of the same sample, with the Chroma q497lp primary dichroic and Chroma HQ 500lp emission filter.

Figure 2-4: The effects of incident laser power on image quality are dramatic, and careful management of laser power is critical to successful imaging of fluorescent probes in living samples. Panels A-C represent images collected from the same field of view within a Bodipy-Fl phallacidin sample (Molecular Probes Fluocell #1). As the power is increased, the image gets brighter, when imaging parameters are kept constant. When the imaging parameters are varied, Panels D-F, a similar quality image is generated by each power level. The consequences of using too much laser power are illustrated in Panel G: three separate regions were exposed to differing amounts of light for 2 minutes each. The 5% power region is essentially undetectable, whereas significant photobleaching has occurred in each of the other regions. Panel G was collected at 0.7 x magnification, with respect to Panels A-F, illustrating the damage done to the sample by collecting images A-F.

Figure 2-5: Several different types of imaging chambers were tested for use with primary neural crest cell cultures. Panel A shows porthole chambers of different configurations, as well as wafer handling forceps (Gelman 30033-042). Standard tissue culture chambers were modified by the Chemistry Machine Shop by boring 15-17 mm holes through the bottom surface. The most common chamber used was the Falcon 35 mm tissue culture chamber (35-3001). When it was desirable to have multiple wells, the Nunc Nunclon 4 well chamber (176-740) was used. Coverslips were secured into these chambers with silicon grease. For ease of coverslip loading, a custom chamber (Herb Adams, Caltech Central Plant) was occasionally used, as in Panel B. For routine imaging of strongly adherent cells, i.e., mouse embryo fibroblasts, LAB-TEK 2 well chambers (Nalge Nunc 155380) were used, as in Panel C.

Figure 2-6: A wide range of GFP fusion proteins were tested in primary neural crest cells. The most useful were actin GFP (Panel A), membrane GFP (Panel B), nuclear GFP (Panel C), and mitochondrial EYFP (Panel D). A-C are images of primary neural crest cells. D is an image of a mouse embryo fibroblast.

Figure 2-7: The timing of neural tube removal from neural tube explant cultures was an important factor in determining the final density of the neural crest cell culture. Each of these images is a representative sample from the same batch of neural tube explant cultures, photographed 46 hours after explanting. The neural tube was mechanically removed with forceps at 6 hours (Panel A), 15.5 hours

(Panel B), or 24 hours (Panel C) after explanting. The observed difference in culture density persisted for days after neural tube removal.

Figure 2-8: A schematic view of the chemistry underlying our photolithographic patterning. Coverslips were first cleaned in a strong acid peroxide solution, then coated in a self-assembled monolayer of aminopropyltriethoxsilane, which served to functionalize the glass surface with a layer of primary amines. This silane layer was then further derivatized with a bifunctional crosslinker 4-benzoylbenzoic aicd, succinimidyl ester (Molecular Probes B-1577). The succinimidyl ester binds to the primary amine within the silane layer, producing a surface of benzophenone groups. Upon irradiation with soft ultraviolet light these benzophenone groups are photoactivated and can insert into C-H bonds in any nearby molecules. Thereby patterned exposure to UV light results in patterned immobilization of proteins on the glass coverslip. Full details of the experimental protocols are available in Appendix 2.

Figure 2-9: Schematic view of the coverslip irradiation procedure. The benzophenone functionalized coverslip was loaded onto a patterned chrome on glass photomask, with a small volume of protein solution in between. The whole glass sandwich was then loaded into a mask aligner in the Roukes Lab at Caltech. The photomask allowed UV light through to the sample in a defined pattern and proteins were preferentially immobilized where the light hit, resulting in a positive patterning process.

Figure 2-10: A comparison of protein patterns generated via two different patterning approaches. Panels A and B present views at two different magnifications of patterns of rhodamine labeled bovine serum albumin on plastic, generated via protein adsorption. There are regions within the sample that are well patterned, but the quality is highly variable. Panels C-E present views at three different magnification of three different patterns of the same fluorescent protein generated by photolithography. These examples are typical of coverslips from a successful patterning batch. Details of the experimental protocols used to generate each batch are presented in Appendix 2.

Figure 2-11: Representative frames from time-lapse movies recording neural crest cell behavior on substrates of ephrin-B1 (red stripes) patterned in stripes against a background of fibronectin. In each case nine frames of the resulting time-lapse movie are presented. Some cells in each field of view appear confined between the stripes and most appear to ignore the pattern. In Panel D, several distinct lines of cells accumulate preferentially on the stripe pattern. The variability in the cellular response was attributed to variations in the patterning and to the heterogeneous nature of neural crest cultures.

Figure 2-12: Details of cell behavior in a ephrin-B1 versus fibronectin neural crest choice assay. Figure 2-12 presents an expanded view of the movie from

Figure 2-11 B. Membrane GFP labeled neural crest cells are cultured on a plastic substrate with adsorbed ephrin-B1 (red stripes) versus fibronectin everywhere. One cell (large arrow) migrates freely across the stripes, without seeming restricted. Another cell within the same field of view (small arrow) appears trapped by the ephrin-B1 stripes and is unable to exit its current lane until a thin projection crosses over into the adjacent lane (Frame 500), whereupon it is able to freely migrate over a domain it had previously found repulsive. Such differences in cellular response made interpreting experimental results very difficult.

Figure 2-13: Stripe assays presented neural crest cells with the choice between migrating in regions of photoimmobilized ephrin-B1 versus fibronectin everywhere. Consistently there were fewer cells in regions of ephrin-B1, but only slightly fewer, and the morphology of cells on stripes was often little different than cells in permissive regions.

Figure 2-14: High-resolution description of cell behavior as a neural crest cell encountered a pattern of ephrin-B1 vs. fibronectin. This individual neural crest appears repelled by contact with ephrin-B1, and extends and retracts pseudopodial projections on the ephrin-B1 surface, only to finally collapse and retract off the stripe. This reaction is very similar in extent and timing to that reported in previous studies with adsorbed stripes of ephrin-B1 [1, 2]. It was very difficult to determine what the typical response of a neural crest cell was; this

reaction was consistently observable, but was not the only observable reaction; many cells seemed different to the imposed photolithographic pattern, particularly if they were in contact with other cells.

Figure 2-16: Vacuum deposition of silane layers onto glass coverslips, followed by adsorption of protein in patterns defined by flow channels, was capable of generating high quality patterns (Panel B). However, variability was still quite high (Panel A). These patterning techniques were adapted from Chris Chen's lab at Johns Hopkins. Details of the experimental technique are given in Appendix 2.

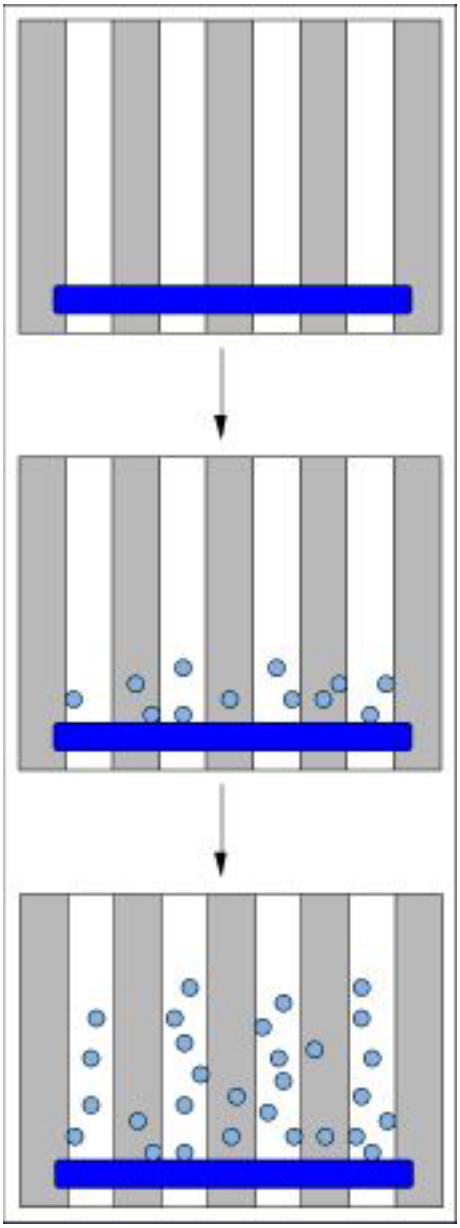

20x Plan Neofluar, 0.5 NA□ 20x Fluar NA 0.75

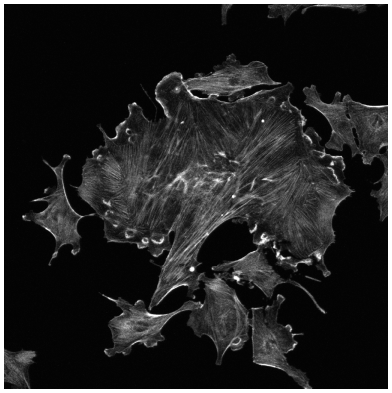

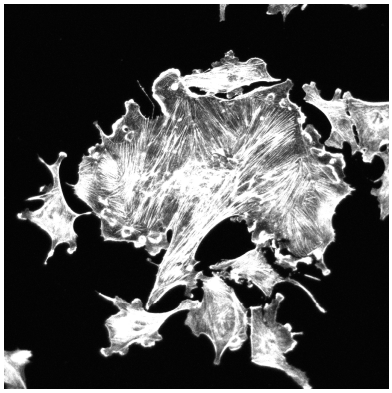

A□ □ □ □ B

40x Plan Neofluar, 0.75 NA □ 40x C-Apochromat, 1.2 NA

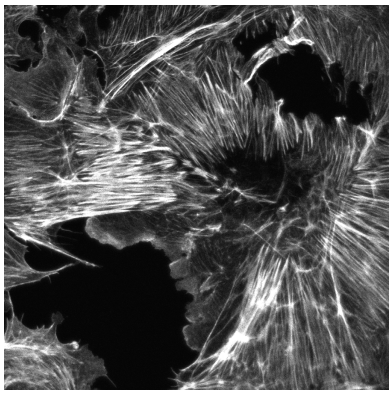

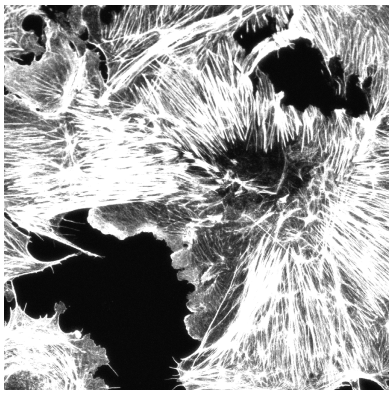

C□ □ □ □ D

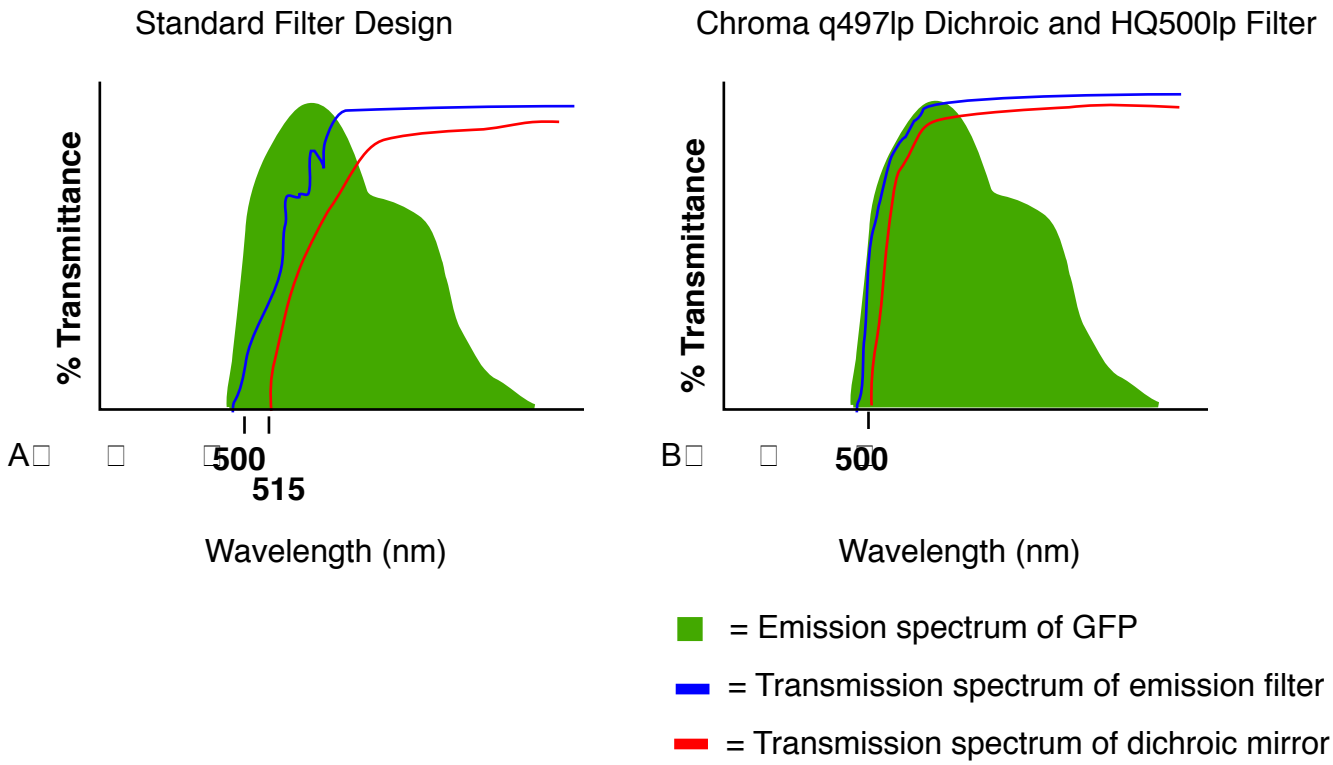
Standard Filter Design
Chroma q497lp Dichroic and HQ500lp Filter
% Transmittance
% Transmittance
500
515
500
Wavelength (nm)
Wavelength (nm)
= Emission spectrum of GFP
= Transmission spectrum of emission filter
= Transmission spectrum of dichroic mirror

A B

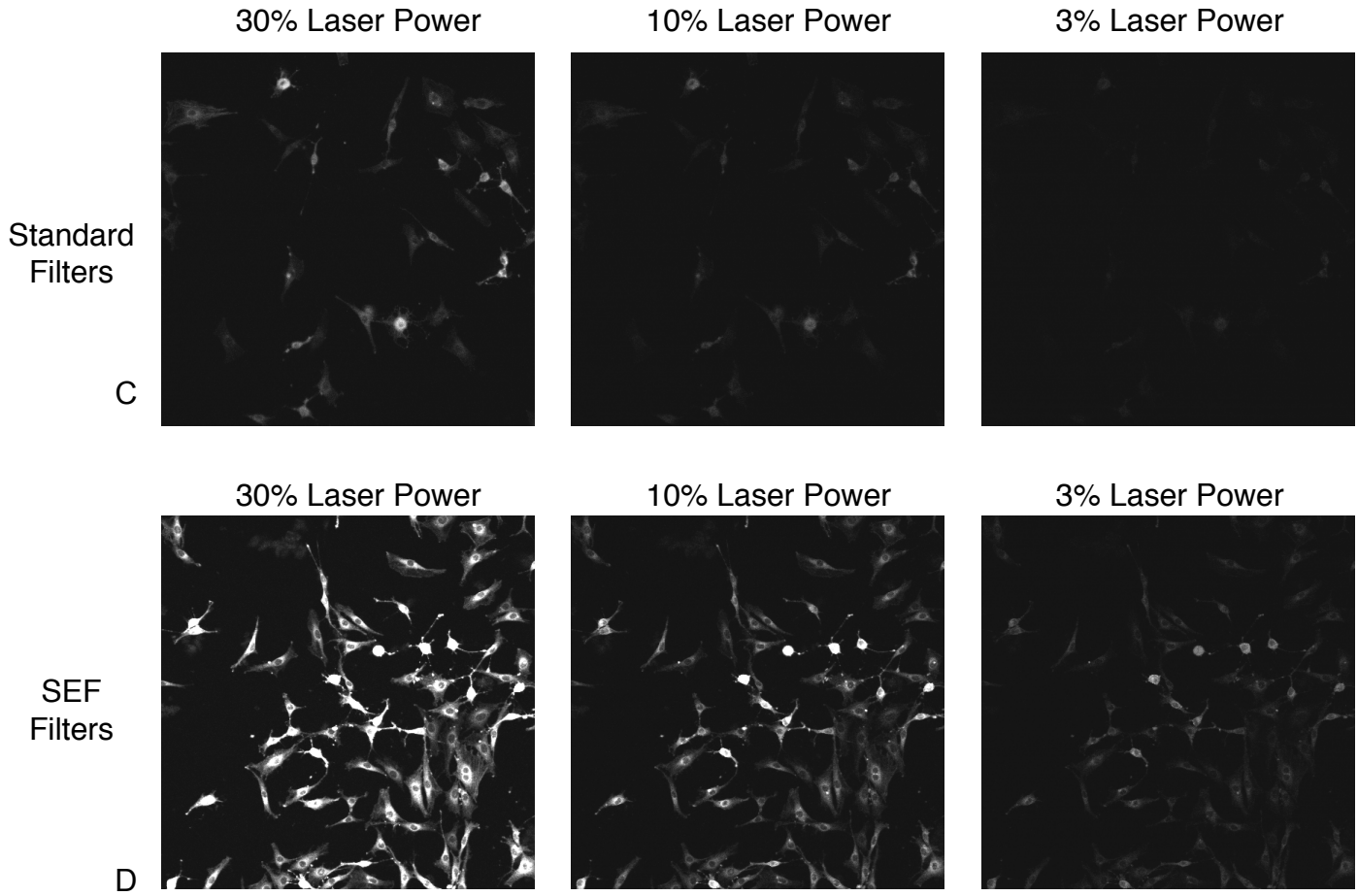
30% Laser Power
10% Laser Power
3% Laser Power
Standard Filters
C
30% Laser Power
10% Laser Power
3% Laser Power
SEF Filters
D

Effect of Power on Image Quality

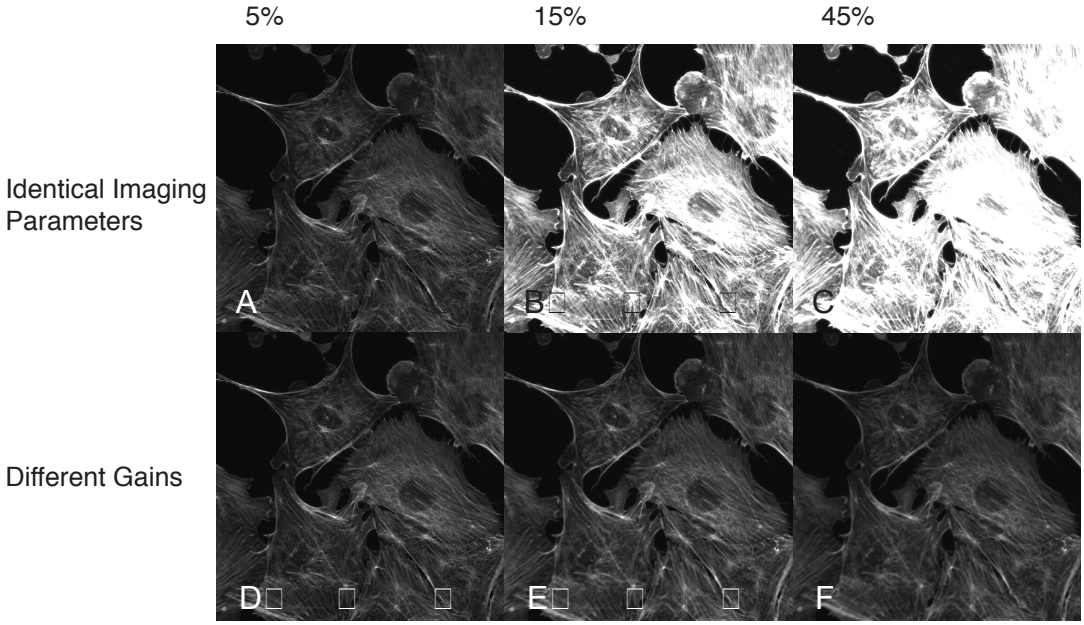

Photobleaching After 2 Minutes of Scanning at Different Power Levels

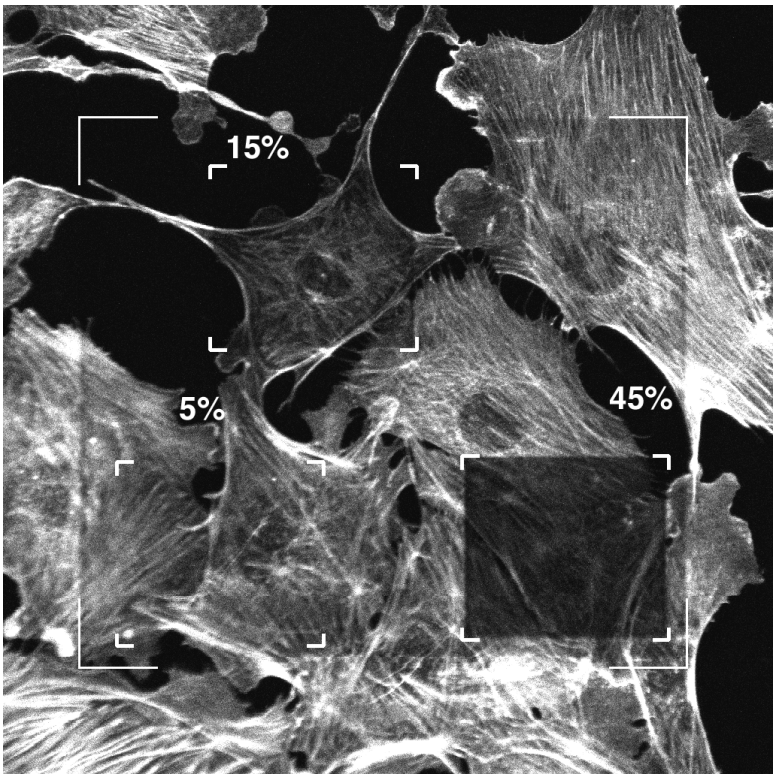

G

A

B

C

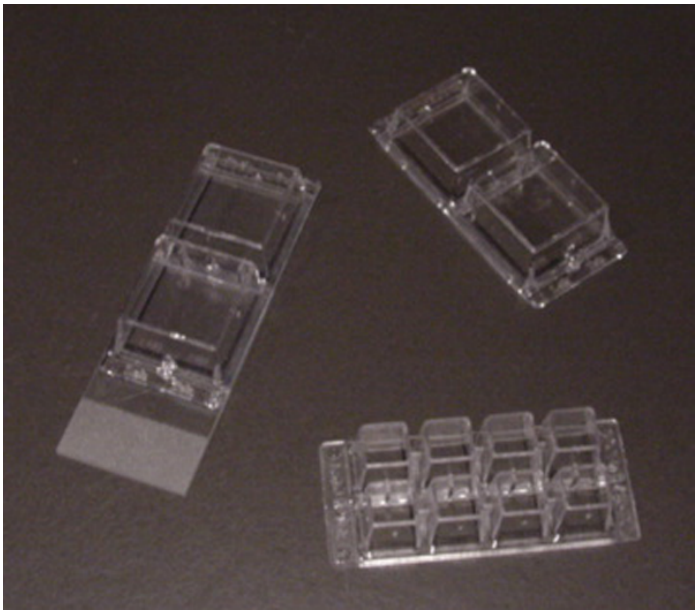

A 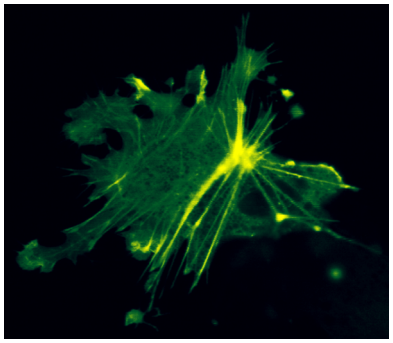

B 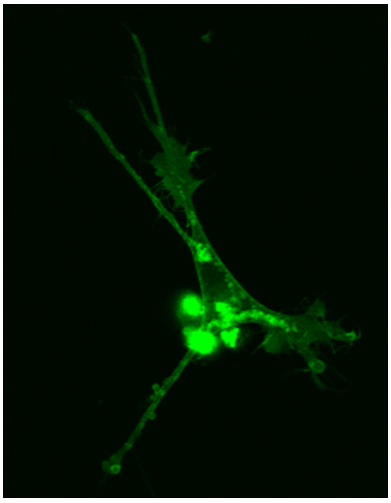

C 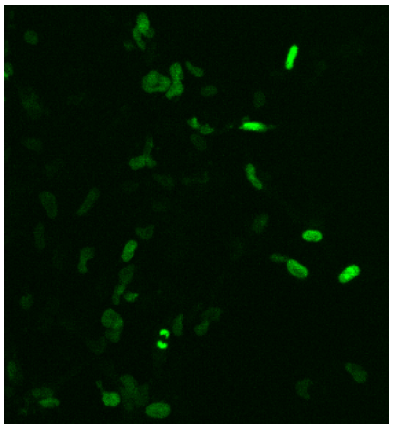

D 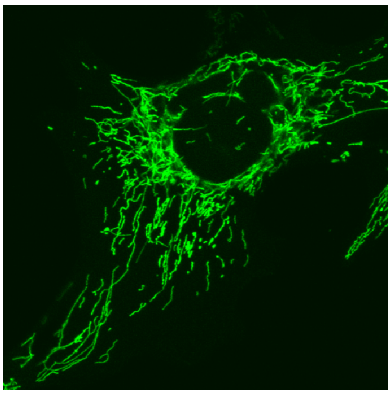

A

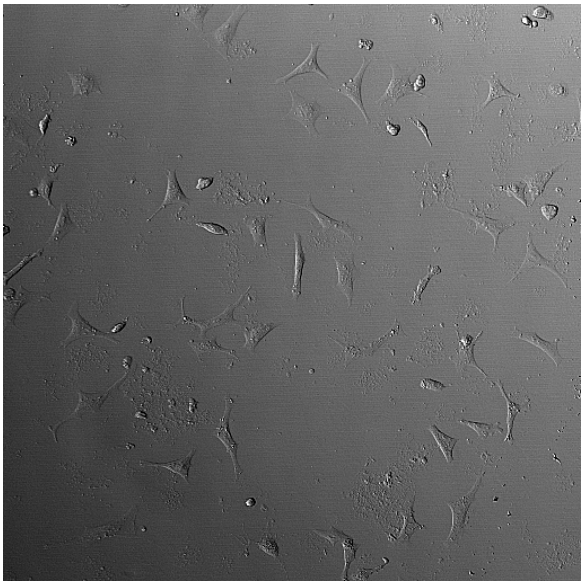

Disperse

B

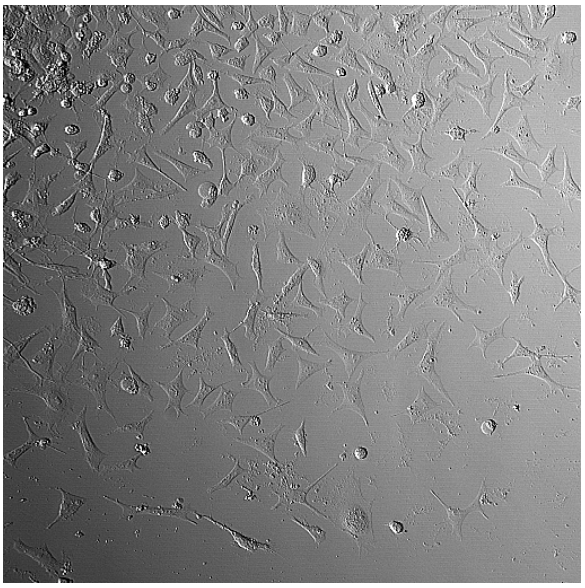

Intermediate

C

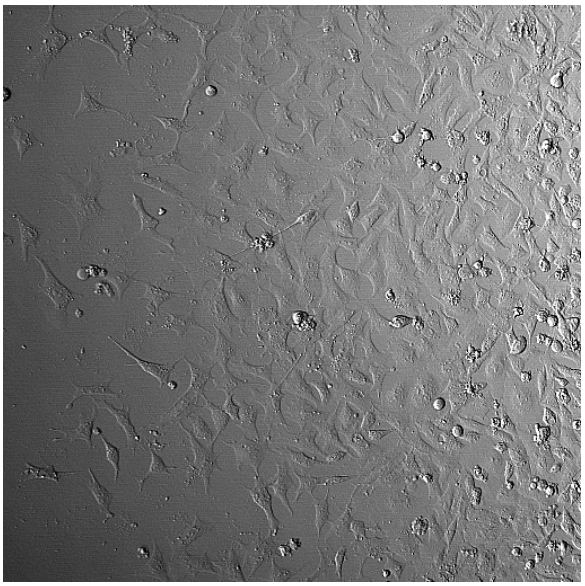

Dense

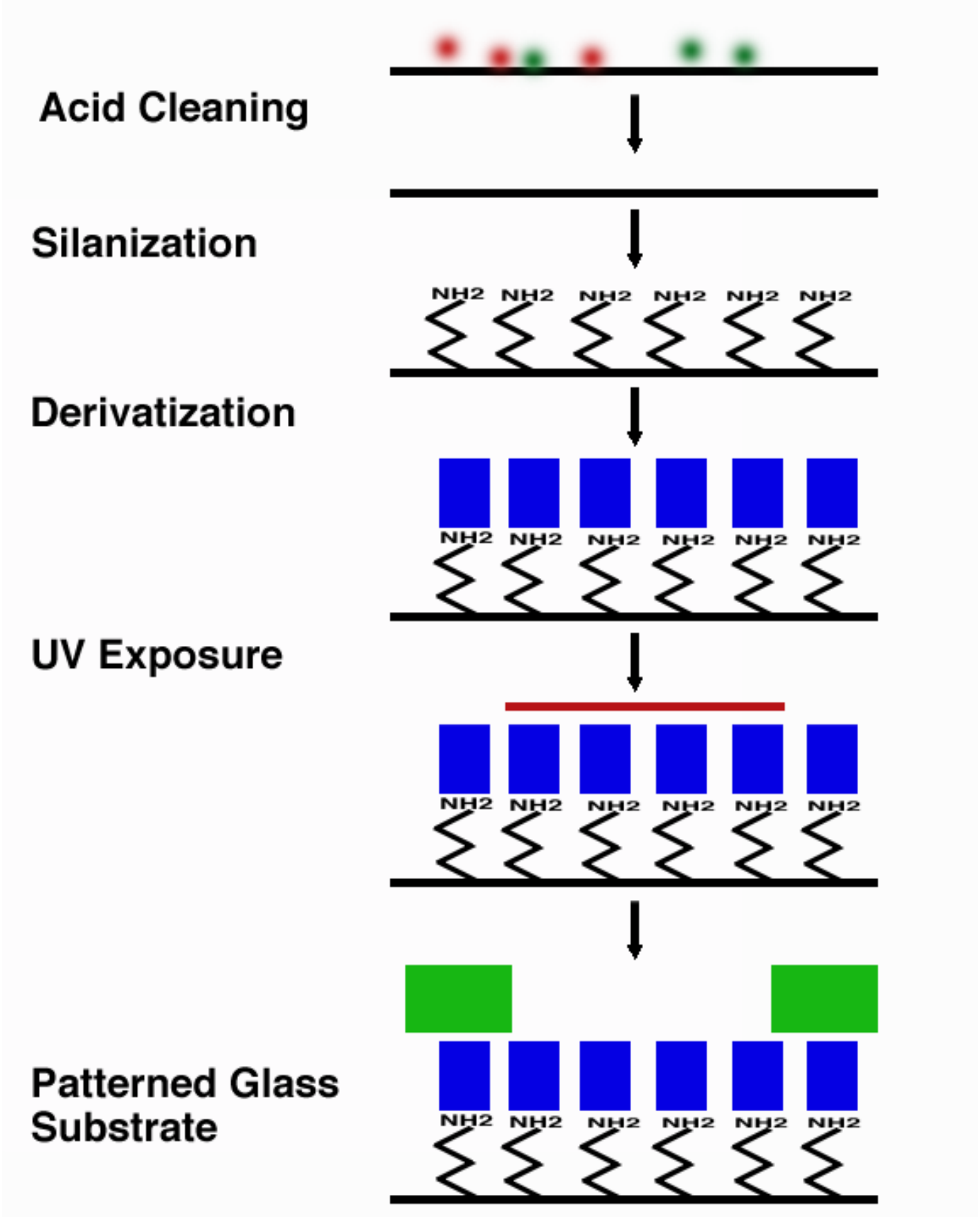
Acid Cleaning
Silanization
NH2 NH2 NH2 NH2 NH2 NH2
Derivatization
NH2 NH2 NH2 NH2 NH2 NH2
UV Exposure
NH2 NH2 NH2 NH2 NH2 NH2
Patterned Glass Substrate
NH2 NH2 NH2 NH2 NH2 NH2

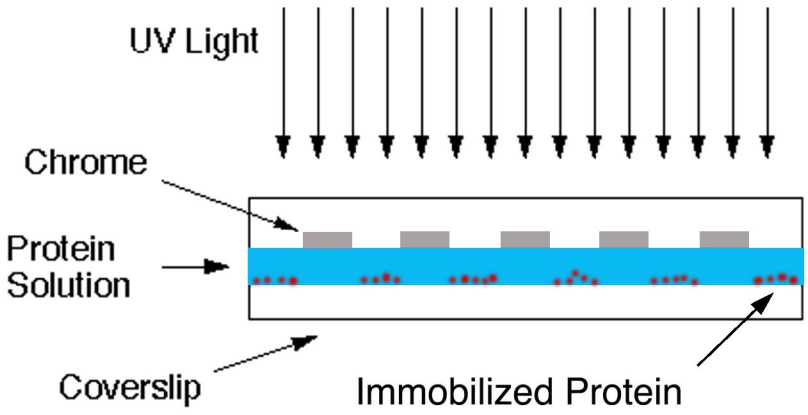
UV Light
Chrome
Protein
Solution
Coverslip
Immobilized Protein

Fluorescent Proteins on Plastic, Generated with Flow Channels

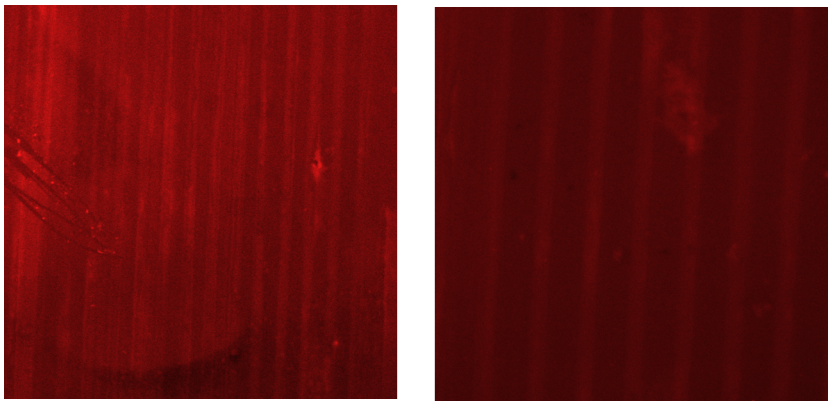

A 250 microns B 125 microns

Photolithographed Fluorescent Protein Patterns

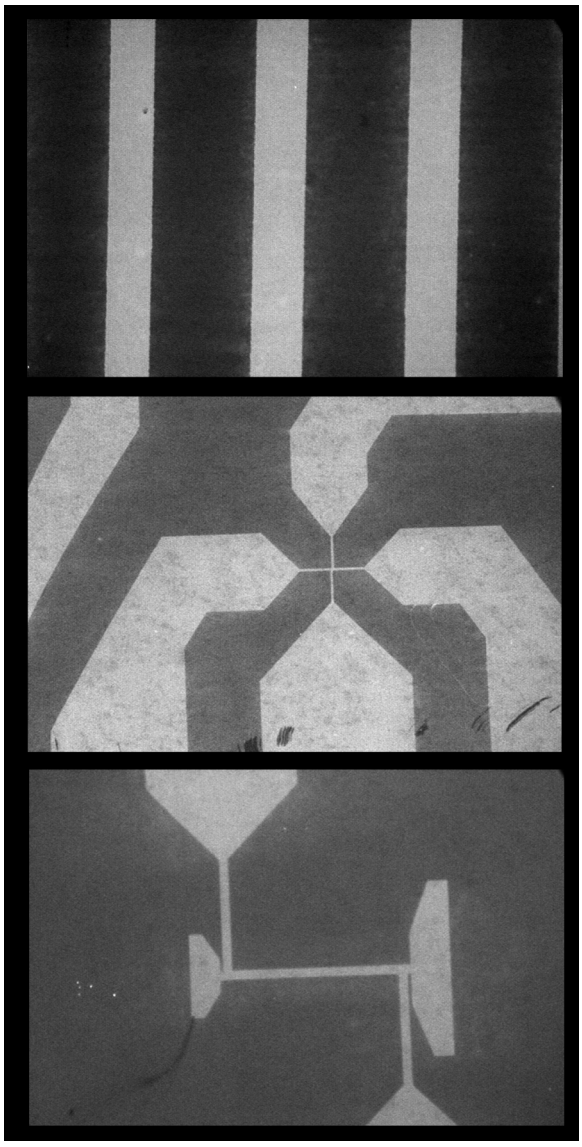

C 10x

D 20x

E 40x

Bonhoeffer style stripe assays: ephrin-B1 vs FN on plastic.

12/12/98-12/14/98

A 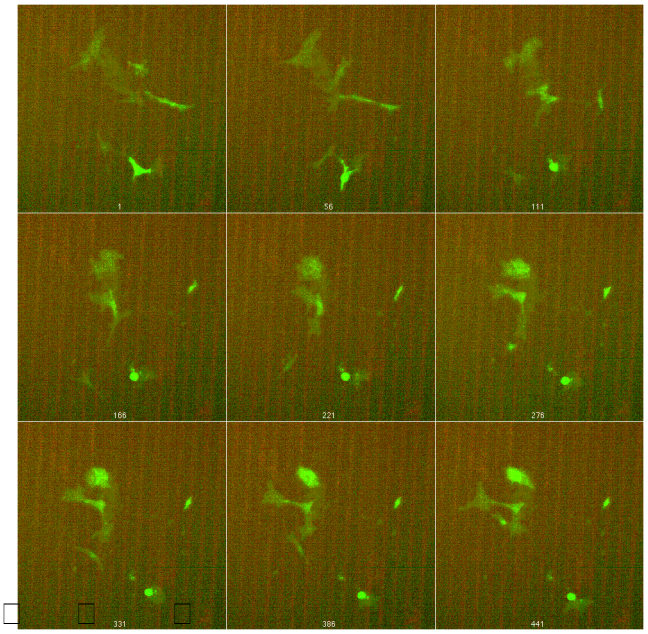

Series 5: 20x, z=1

B 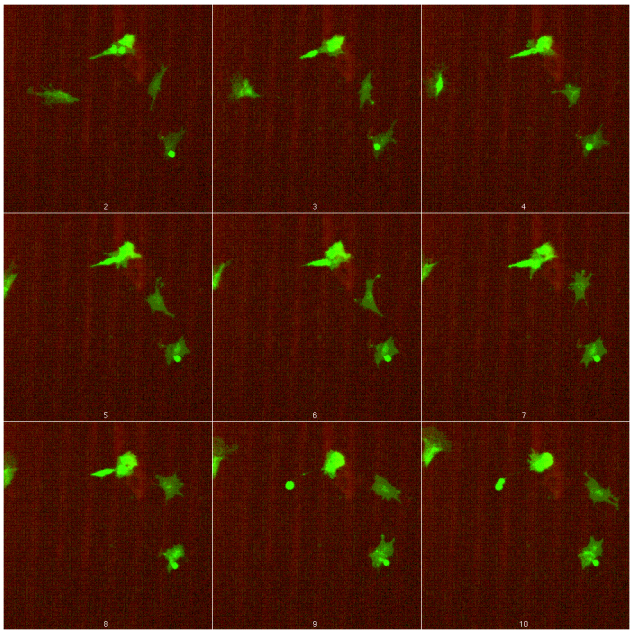

Series 6: 20x, z=1

C 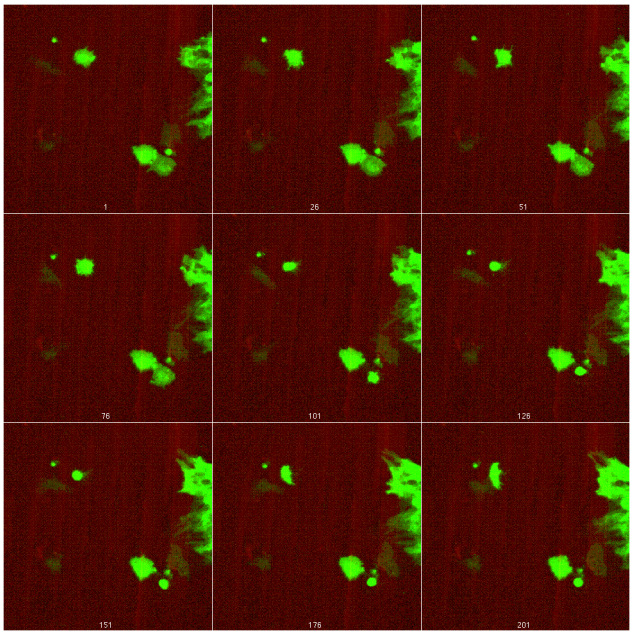

Series 7: 20x, z=1

D 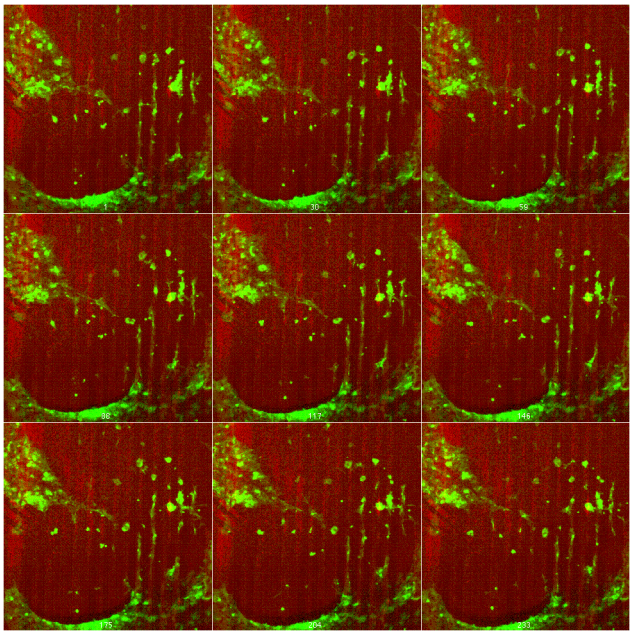

Series 8: 10x, z=1

Membrane GFP Time Lapse of Neural Crest Cells on a Pattern of ephrin-B1 vs. Fibronectin
Series 6, Gap43-GFP, 20x, 900 images, taken every 30s 12/13/98

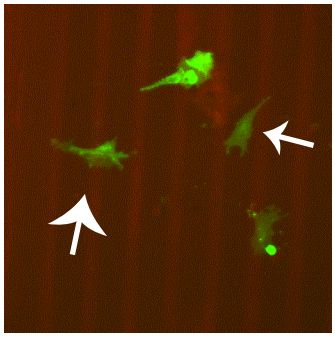

Frame 100

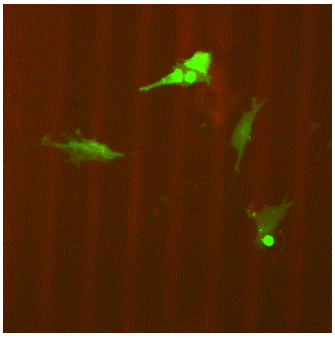

Frame 150

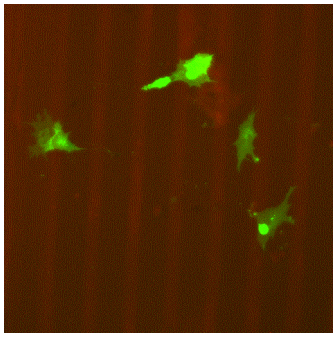

Frame 300

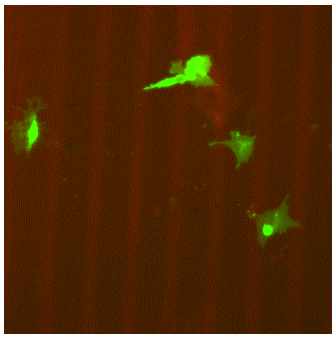

Frame 360

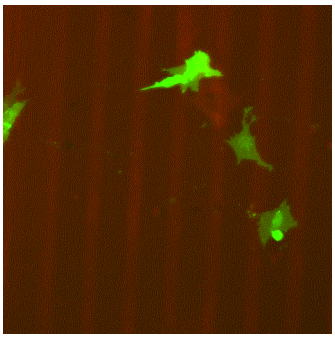

Frame 500

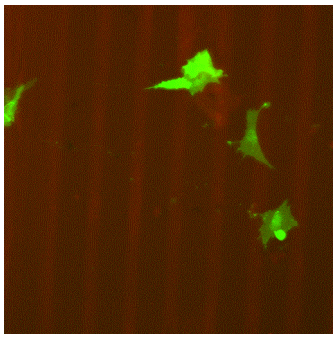

Frame 550

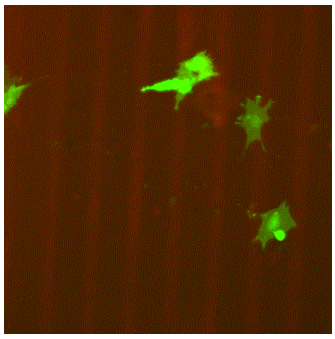

Frame 613

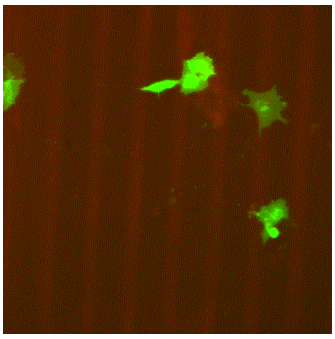

Frame 680

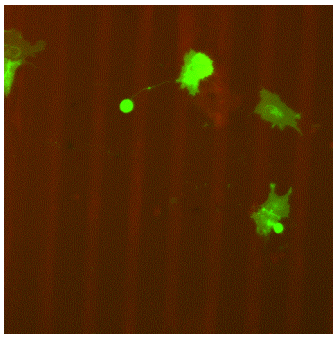

Frame 800

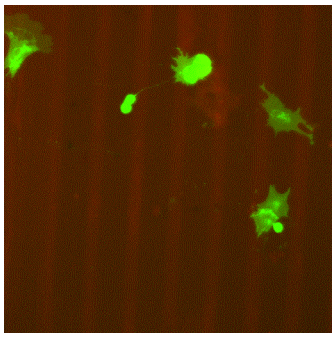

Frame 867

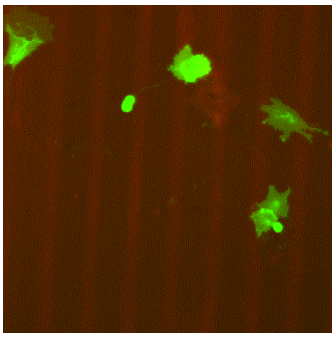

Frame 900

Neural Crest Cells on Photolithographed ephrin-B1 Striped Substrates
Red Shading Indicates ephrin-B1 Containing Area 2/21/00

A

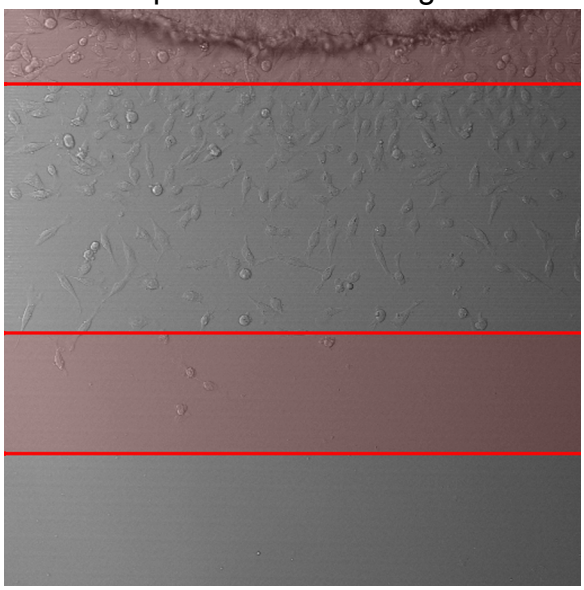

B

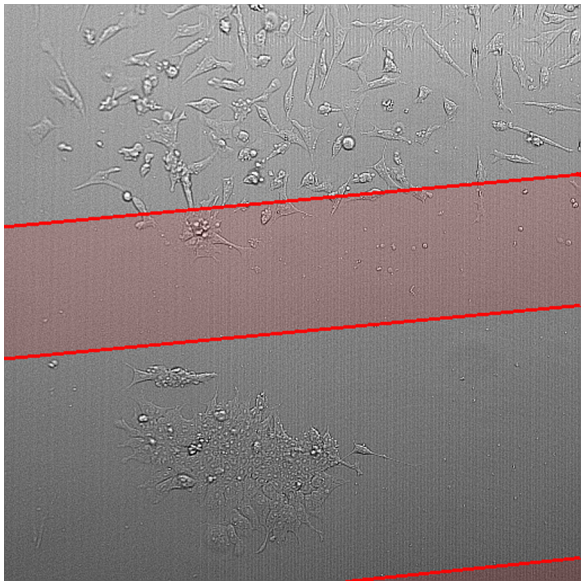

C

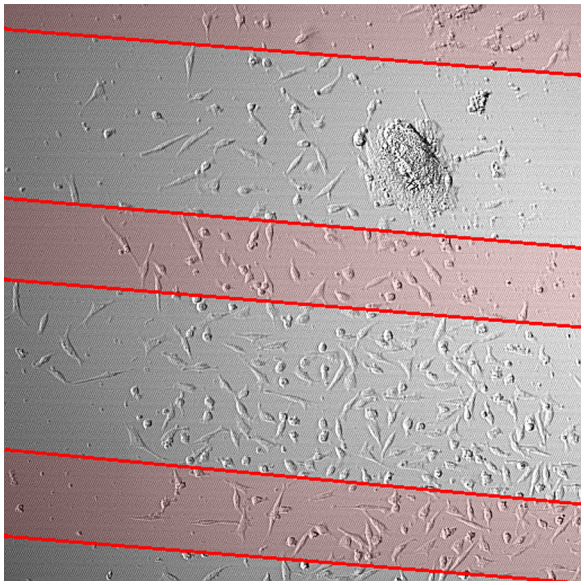

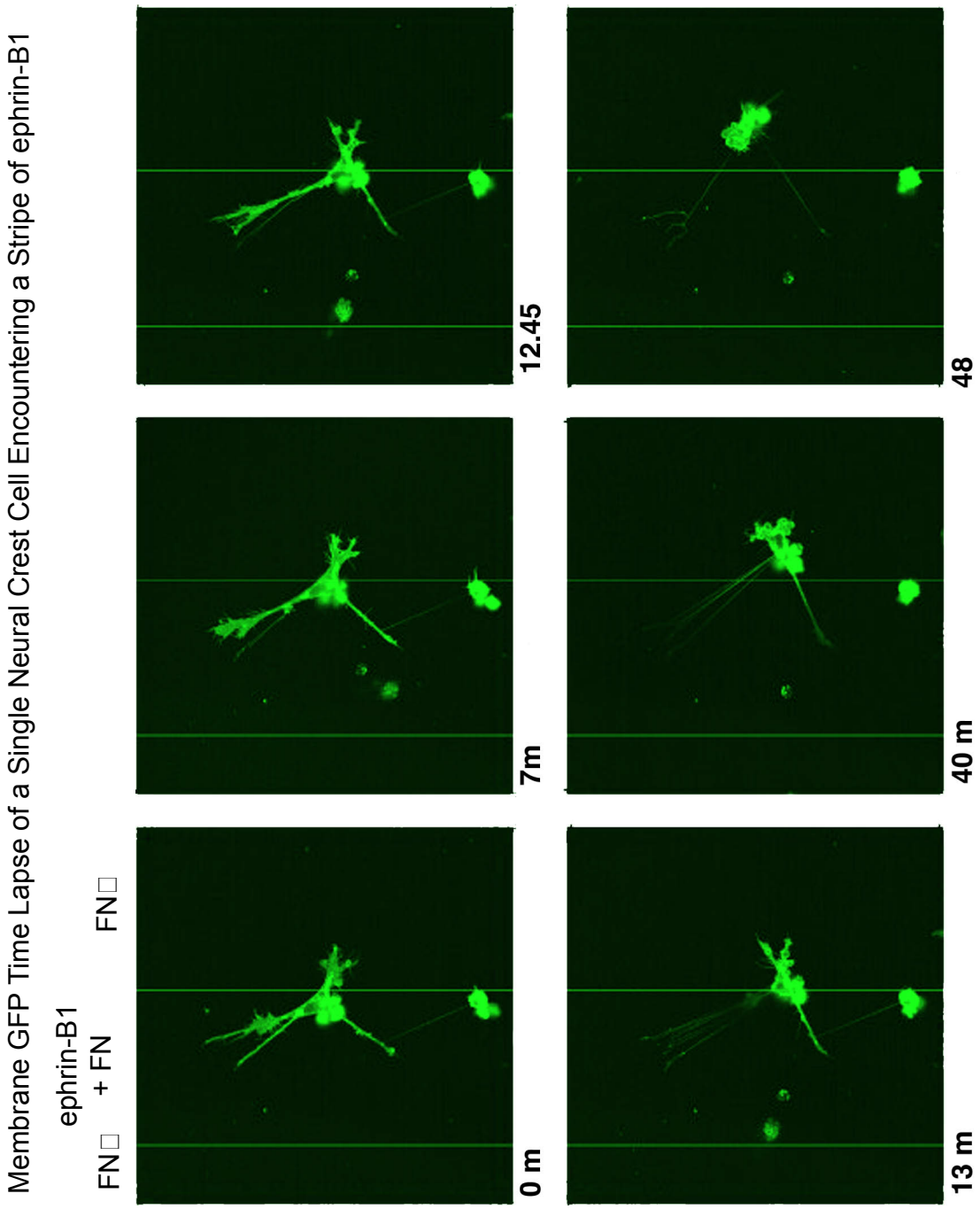
Membrane GFP Time Lapse of a Single Neural Crest Cell Encountering a Stripe of ephrin-B1
ephrin-B1
FN□
+ FN
FN□
0 m
7m
12.45
13 m
40 m
48

Patterns of Fluorescent Proteins on Vacuum Deposited Silane Surfaces

A 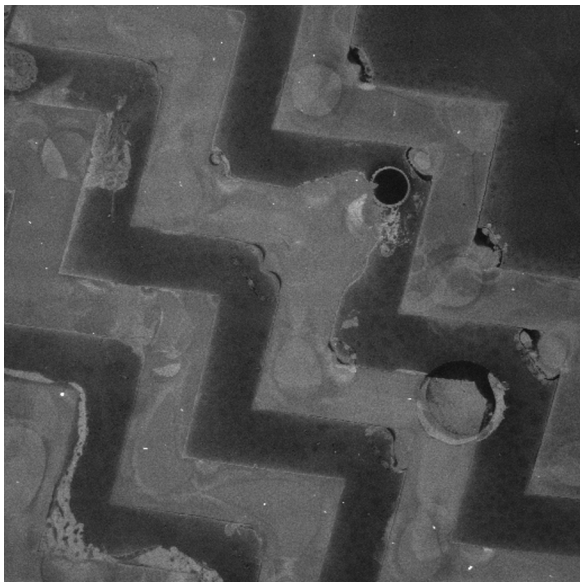

B